Grinding Kinetics of Vanadium-Titanium Magnetite Concentrate in a Damp Mill and Its Properties

HONGMING LONG, TIEJUN CHUN, PING WANG, QINGMIN MENG, ZHANXIA DI, and JIAXIN LI

The grinding behavior of the as-received (5 pct moisture) vanadium-titanium magnetite concentrates in a damp mill was investigated in this paper. A grinding kinetics equation was established based on a population balance model using size distribution data obtained from a laser diffraction technique. X-ray diffraction results show that a loss in crystallinity occurs when the grinding time is increased. The crystallite size of the materials decreased, whereas their structural microstrain increased with increasing grinding time. The wettability increased because the surface roughness increases with increasing grinding time. The moisture capacity of the solids increased during the first 3 minutes of grinding and then remained roughly constant with further increases in grinding time. The water transfer coefficient of the particles increased at grinding times of 3 and 6 minutes and then decreased at grinding times of 9 and 12 minutes. The compressive strength of oxidized pellets increased with increasing grinding time; longer grinding times can compensate for the effects of lower roasting temperature or shorter roasting time on the strength of the pellets. Lowering the roasting temperature and shortening the roasting time by grinding appeared to be possible.

DOI: 10.1007/s11663-016-0644-7

I. INTRODUCTION

PELLETIZATION is desirable for the agglomeration of fine concentrates because the particles are normally of such fine size that they form into a green ball with little difficulty. Coarse ores that have unsuitable sizes require grinding prior to pelletization. The specific surface area and surface activity of ores can be enhanced by grinding, which also improves their pelleting efficiency.[1–3] Vanadium–titanium magnetite (VTM) ore, a special iron ore composed of about 12 pct TiO_2 and 0.1 pct V_2O_5, is the beneficiation product of deposits in Panzhihua, China. VTM has poor wettability and is difficult to granulate prior to sintering. Grinding in damp mills has been reported to improve the agglomeration ability of the ore, which is the main objective of the current study. In this work, the grinding kinetics, surface morphology, lattice distortion, wettability, and moisture capacity of VTM concentrates ground for different times were analyzed. The compressive strength of finished pellets produced with and without grinding was also analyzed.

HONGMING LONG, PING WANG, and JIAXIN LI, Professors, TIEJUN CHUN and QINGMIN MENG, Associate Professors, and ZHANXIA DI, Lecturer, Professor, are with the School of Metallurgical Engineering, Anhui University of Technology, Ma anshan, 243002, China. Contact e-mail: springcsu@126.com
Manuscript submitted September 28, 2015.
Article published online March 21, 2016.

II. MATERIALS AND EXPERIMENTAL METHODS

A. *Raw Materials*

The original water content of the raw materials was 5.05 pct. The chemical composition of the VTM concentrate is presented in Table I. The mass percentages of TFe, TiO_2, and V_2O_5 in the VTM were 53.97, 12.77, and 0.56 pct, respectively. Figure 1 shows the size distribution of the VTM concentrate. The mass fraction of particles under 200 mesh in size was about 50 pct, which is unsuitable for pelletization.

B. *Experimental*

All materials were ground at the as-received moistures (5.05 pct). The grinding machine was a laboratory scale damp mill with rubber liners. The inside diameter and inner volume of the mill chamber were 0.5 m and 0.1 m^3, respectively. Steel balls were used as the grinding media, and the rotational speed of the mill was set to 48 rpm. When the mill was rotated, the medium and ore, also known as the mill charge, were mixed well. The medium comminuting the particles depended on the rotation speed of the mill and the shell liner materials. Control of product size was exercised based on the type of medium used, the rotation speed of the mill, and the grinding time. In the current study, six groups of experiments were performed to compare the effects of different grinding times (3, 6, 9, 12, 30, and 60 minutes) on pellet strength. The feed sample mass was 5 kg in all cases. After grinding, the materials were immediately dried at 393 K (120 °C) for 2 hours to ensure that they

Table I. Chemical Composition of Vanadium-Titanium Magnetite

Item	TFe	FeO	CaO	SiO_2	MgO	Al_2O_3	TiO_2	V_2O_5	MnO	S	P
Mass Pct	53.97	20.89	1.13	3.38	2.73	4.18	12.77	0.56	0.37	0.74	0.004

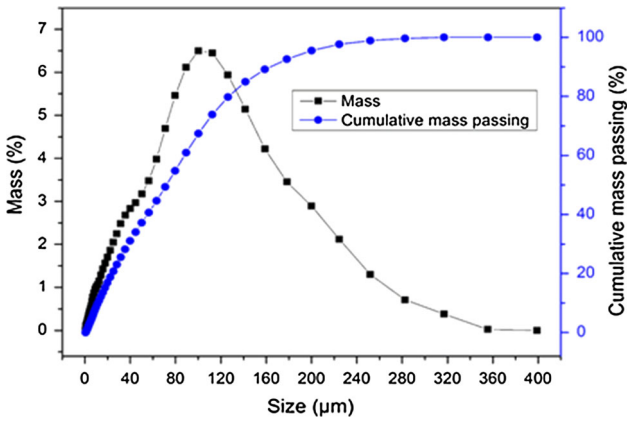

Fig. 1—Size distribution of vanadium-titanium magnetite.

were completely dry, and the size distribution of particles was measured using laser diffraction method. The laser diffractometer used in this study was an MS 2000 system (Malvern Instruments), and its valid measurement range was from 0.02 to 2000 μm. Scanning electron microscopy (SEM) was used for mineralogical observation. Crystallite sizes and structural microstrains were measured by X-ray diffraction (XRD) using a Rigaku Ultima X-ray diffractometer and Cu K_α radiation. The wettability of ores was characterized based on the contact angle between the ores and water using the penetration method.[4] The moisture capacity of the samples was also measured in this study. The preparation of green pellets and the measurement of green pellets and roasted pellets were according to the references.[5,6] The Bond grindability test for determining the Bond work index W_i is conducted in a Bond ball mill having the dimensions $D \times L = 305 \times 305$ mm and a speed revolution of 70 min^{-1}. The mill is loaded with balls from 15.5 up to 30.6 mm in diameter, having thus a total mass of 20.125 kg. This test simulates a closed circuit of dry grinding of samples of standard size in the range of 0 to 0.4 mm, leading to the point of achieving a circulating load of 250 pct.

III. CHARACTERIZATION OF THE PARTICLES

A. *Grinding Kinetics and Bond Word Index*

Figure 2 shows particle size distributions of the products obtained from various grinding times in the mill. The dependence of the median particle size (x_{50}), as well as mean volume diameter D (4, 3) and specific surface area S_{LS}, on the grinding time is presented in Figure 3. With increasing grinding interval, the size distribution curve shifted toward the left. When the grinding time reached 30 minutes, another subpopulation appeared at approximately 32 to 34 μm; this subpopulation is believed to be induced by particle agglomeration.[7]

Figure 3 shows the evolution of the median diameter and specific surface area of the particles as a function of time. The particle size decreased rapidly during the first 3 minutes of grinding and then appeared to slow down. After 30 minutes, the median size approached a constant value, probably resulting from equilibrium between the fragmentation and the agglomeration processes. During the first 12 minutes of grinding, the specific surface area, which was calculated using the laser diffraction method, increased with the grinding time; however, it remained basically invariable with further increasing grinding time. This phenomenon indicates that agglomeration takes place within a few minutes of milling, and the results agree with the evolution of experimental size distributions *vs* grinding time (Figure 2). Another subpopulation appeared when the grinding time reached 30 minutes.

Grinding kinetics is commonly described using population balances, which are modeled using a classical batch-grinding equation based on selection and breakage functions. The change in particle size distribution of ground material is described as a function of grinding time, t, as follows:[8,9]

$$\frac{\partial^2 D(x,t)}{\partial t \partial x} = -\frac{\partial D(x,t)}{\partial x} S(x,t) + \int_x^{x_m} \frac{\partial D(\gamma,t)}{\partial \gamma} S(\gamma,t) \frac{\partial B(\gamma,x)}{\partial x} \mathrm{d}\gamma, \quad [1]$$

where $D(x, t)$ is the cumulative undersize of particles x, t is the grinding time, x is the size of a single particle to be broken, and x_m is the maximum particle size present. Assuming $S(x,t) = Kx^n$, and $B(\gamma,x) = (x/\gamma)^m$, where K is the grinding rate constant, and m and n are the exponents, respectively, Eq. [1] can be analytically integrated into the following form with $R(x,t)$ as the cumulative oversize:[10]

$$R(x,t) \approx R(x,0) \exp(-(\mu K x^n t)^v), \quad [2]$$

where μ and v are determined from the ratio of m to n. By considering the application of fine grinding kinetics and from having no theoretical base in general, Eq. [2] can be picked up to analysis of grinding data. Assuming that $K' = (\mu K)$, and $n' = nv$, Eq. [2] can be expressed as follows:

$$R(x,t) \approx R(x,0) \exp(-K' x^{n'} t^v). \quad [3]$$

To obtain the grinding rate constant K' and exponents n' and v, Eq. [3] is converted to

$$\ln\left[-\ln\frac{R(x,t)}{R(x,0)}\right] = n' \ln x + \ln K' t^v, \quad [4]$$

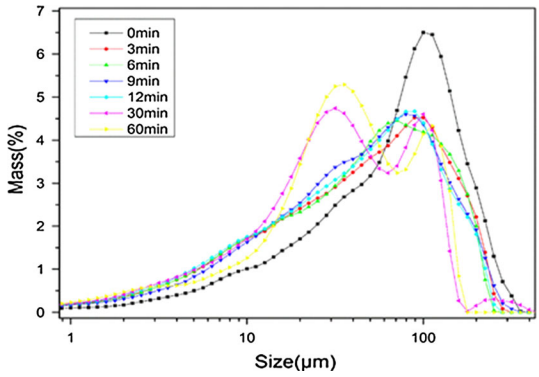

Fig. 2—Particle size by laser size analyzer for ores studied.

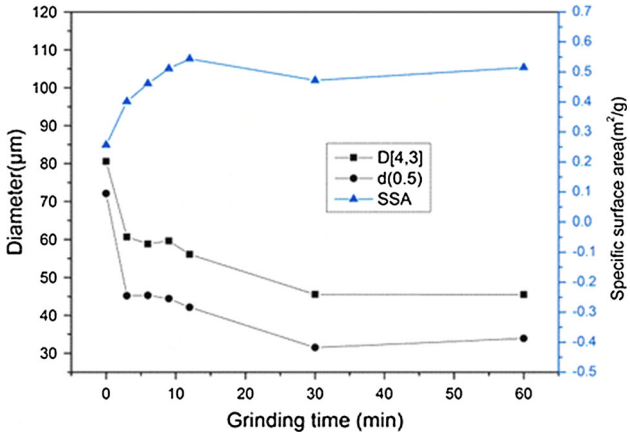

Fig. 3—Diameter and specific surface area *vs* grinding time.

$$\ln K' t^{v} = v \ln t + \ln K'. \quad [5]$$

The grinding rate constant K' and exponents n' and v can be obtained by regression analysis of the experimental data of particle size distribution using Eqs. [4] and [5]. Figure 4 shows the linear dependence of the normalized cumulative oversize functions on the logarithm of the particle size obtained from different grinding times. The linear dependence of the normalized cumulative oversize functions on the logarithm of the particle size, ln$x$, exists only for data corresponding to grinding intervals of 3, 6, 9, 12, 30, and 60 minutes. Regression analysis of data corresponding to grinding intervals of 3, 6, 9, 12, 30, and 60 minutes using the least-squares method resulted in a constant slope value, n' (0.95), and an intercept, ln $K't^{v}$, that varied with time. The y-intercepts of the straight lines in Figure 4 for grinding intervals of 3, 6, 9, 12, 30, and 60 minutes are plotted against the grinding time in Figure 5. Parameters v and K' were then obtained from linear regression analysis of Eq. [5]. Grinding kinetics analysis of the experimental data resulted in an equation that is suitable for predicting particle size distributions during VTM concentrate grinding using a planetary damp mill:

$$R(x,t) \approx R(x,0) \exp\left(-0.0056 x^{0.95} t^{0.19}\right). \quad [6]$$

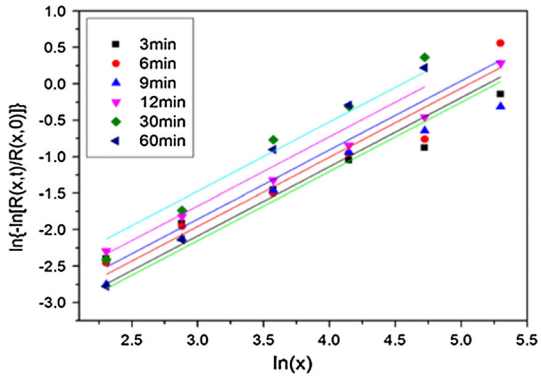

Fig. 4—Relationship between normalized oversize and particle size.

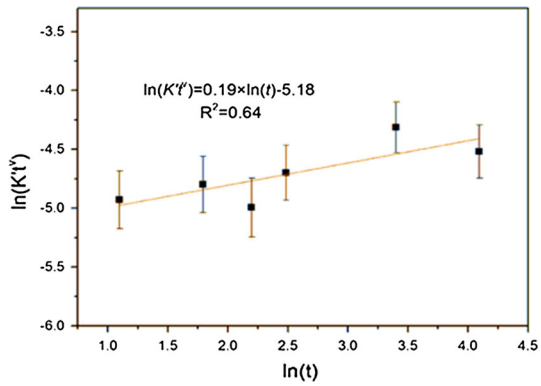

Fig. 5—Variation of intercept ln($K't^{v}$) with grinding time.

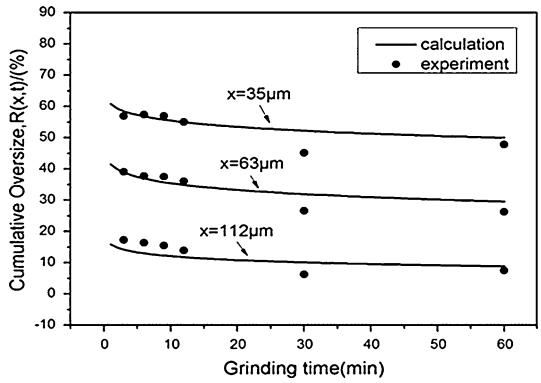

Fig. 6—Comparison of the calculated and measured cumulative oversize.

The good agreement between the experimental and calculated size distributions in Figure 6 confirms the applicability of Eq. [6] to the description of VTM fine grinding.

The size of VTM is 42 pct passing 0.075 mm (Figure 1), with a specific surface area of 0.25 m^2/g (Figure 3). It is necessary to reduce the particle size even more (about 80 to 85 pct passing 0.075 mm), and obtain adequate specific surface area of 0.35 to 0.5 m^2/g for improving the pelletizing process.[11] As shown in Figure 3, the targets of grinding size and specific surface

area are achieved after grinding 3 minutes. In order to estimate the grinding cost, the Bond work index was also investigated. The Bond work index test has the advantage of being based on a larger volume (700 ml) and with a variable target size, so the impact of target particle size on the grindability of materials can be investigated. The output of the Bond work index test is also in a more useable form of energy consumption per ton (KWh/t), which is defined according to the following calculating equation:[12]

$$W_i = \frac{49.05}{P^{0.23} \cdot G_{bp}^{0.82} \cdot \left(\frac{10}{\sqrt{P_{80}}} - \frac{10}{\sqrt{F_{80}}}\right)}, \quad [7]$$

where P is the aperture of the comparative screen (μm), G_{bp} is the net mass of the newly screened undersize produced per mill revolution (g), the average value from the last three grindability tests, P_{80} is the d_{80} size of the mill product (μm), and F_{80} is the d_{80} size of the mill feed (μm). Table II shows the Bond work test results for VTM, and the W_i of 52.86 KWh/t was obtained.

B. *Surface Morphology*

Figure 7 illustrates the morphological evolution of non-ground and ground particles with increasing grinding time. The first row shows micrographs of the VTM concentrate at 100× magnification. The particle size abruptly decreased when the grinding time reached 30 minutes. The second row shows micrographs at 1000× magnification. The surface morphology of the particles became slightly coarser as the grinding time reached 12 minutes. SEM micrographs further showed an extremely rough surface on particles ground for 30 and 60 minutes. By contrast, agglomerates of fine particles or resulting from the coating of fine particles on coarser fragments were observed when the grinding time was 12 minutes. The agglomerates are easily identifiable on the SEM photos by their brightness because agglomerates present a great number of facets compared with fragments.[13]

C. *Crystallite Size and Structural Microstrain*

The XRD patterns of VTM concentrate with and without grinding for various times are presented in Figure 8. Comparison of the peaks in the diffraction patterns between 25 deg and 65 deg (2θ) shows that the heights of VTM concentrate diffraction peaks decrease and the lines broaden after mechanical activation. Two factors may explain this phenomenon: decreasing crystallite size and enhanced strain in the lattice of the domains.[14] The crystallite size is the effective size of the coherent diffracting domains within a polycrystalline specimen. Microstrain calculations determine the degree of distortion present in crystallites. Since the experimental peak profile consists of the instrumental and intrinsic profiles, instrumental broadening should be removed from the experimental profile to obtain the intrinsic profile. After obtaining the intrinsic profile, the crystallite size and structural microstrain of particles in the presence of size and strain broadening (caused by damp milling) can be determined using Cauchy–Cauchy calculations (Williamson–Hall procedure).[15–18] The crystallite size and microstrain of concentrates obtained at different grinding times are presented in Figure 9. The crystallite size of materials decreased, whereas their structural microstrain increased as the grinding time increased. After 60 minutes of milling on the sample, the crystallite size of the concentrate decreased from about 673 nm to about 510 nm, whereas its structural microstrain increased from 0.031 pct to about 0.048 pct. Because of milling, some of the energy in the mixture induces an increase in internal mixture stresses, which subsequently decreases the crystallite size and increases the structural microstrain.

D. *Wettability*

The surface wettability and shape of VTM concentrate powders have great influences on the pelletization property of the material. The better the wettability of the material, the stronger the capillary force between powders. Contact angles between iron and water are used to characterize the wettability of iron ore particles. In this work, the contact angles of the ores are determined using their liquid penetration rate.[19,20] Figure 10 shows the contact angle of the VTM concentrate after 3 minutes of grinding. The curves represent pressure differences between cyclohexane and water as a function of time, respectively. Approximate lines represent the square of the pressure difference *vs* time, and the slopes are used to calculate contact angles. Table III shows contact angles of the four iron ores calculated using Eq. [8]:[19,21,22]

$$\theta_1 = \arccos\left(\frac{K_1 \eta_1 \gamma_0}{K_0 \eta_0 \gamma_1}\right), \quad [8]$$

where K_0 and K_1 represent the two slopes measured by cyclohexane and water, respectively; γ_0 and γ_1 are the surface tension of cyclohexane and water, respectively; and η_0 and η_1 are the viscosity of cyclohexane and water, respectively. Table II shows that the contact angle between the VTM concentrates and water decreased with increasing grinding time. The value changed in a large range. The original VTM concentrate showed a contact angle (71.42 deg) higher than that of hematite because of its highly hydrophobic surface, which leads to poor water wettability. After grinding, the contact angle of the VTM concentrate decreased slightly. An exponential quadratic equation was established by fitting the experimental data ($\theta = 42 \times 0.96^t + 29$), and the correlation coefficient obtained was larger than 0.98 (Figure 11). The contact angle between the VTM concentrate and water decreased as the grinding time increased. This phenomenon agrees well with the finding that the contact angle decreases when the roughness factor is increased.[23]

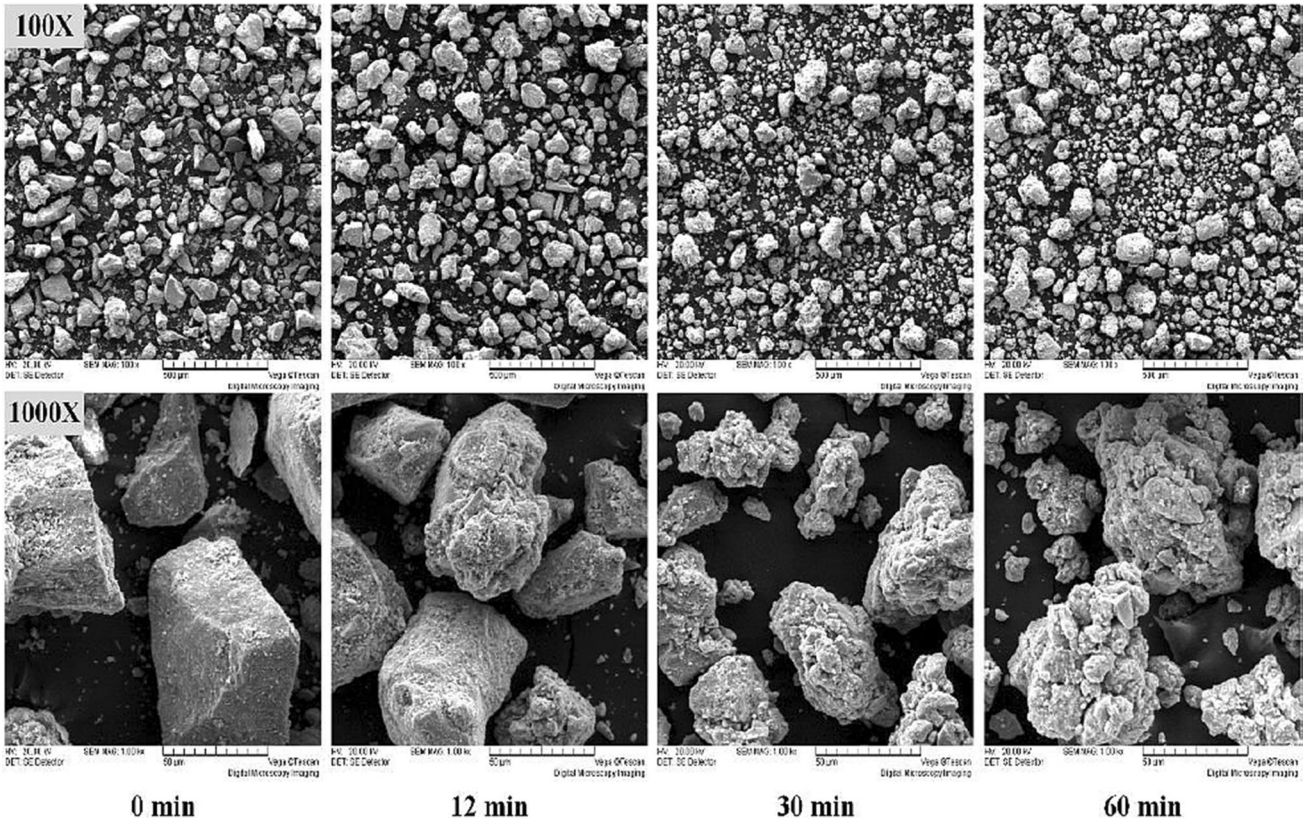

Fig. 7—Micrographs (SEM) of iron ores studied. Here after 0 min refers to the initial sample or non-activated sample.

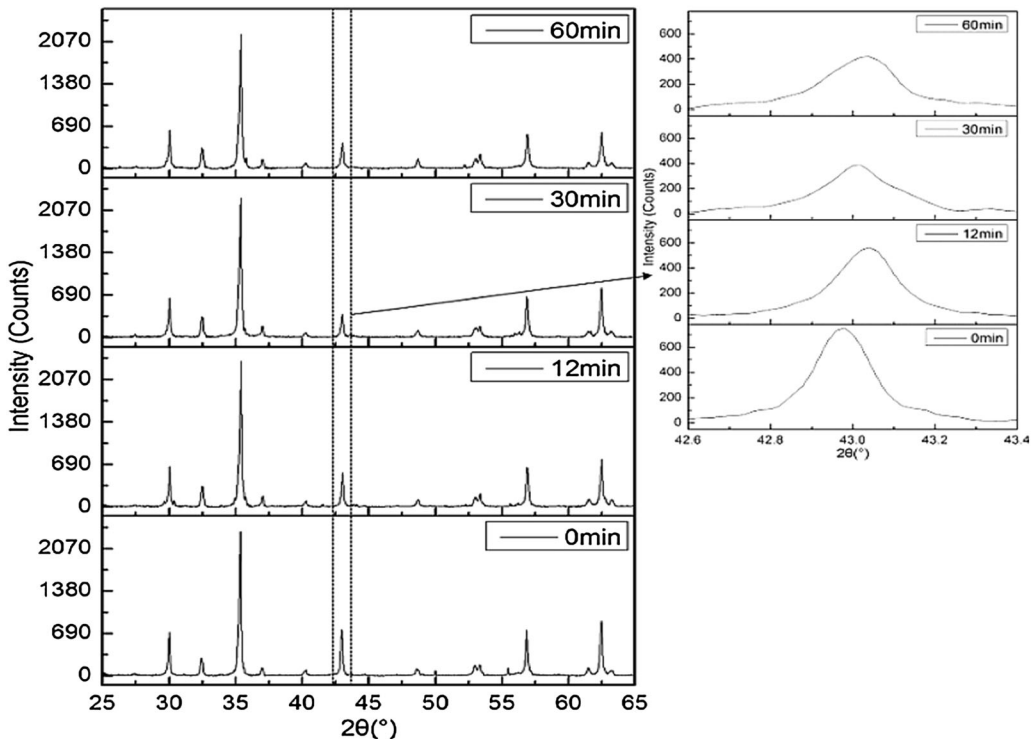

Fig. 8—X-ray diffraction analysis at different grinding times.

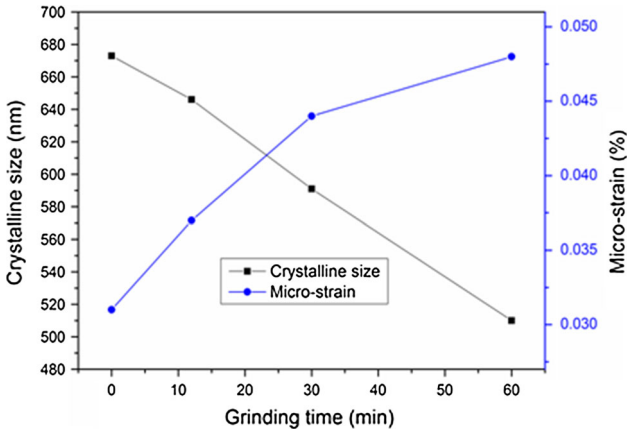

Fig. 9—Crystalline size and microstrain *vs* grinding time.

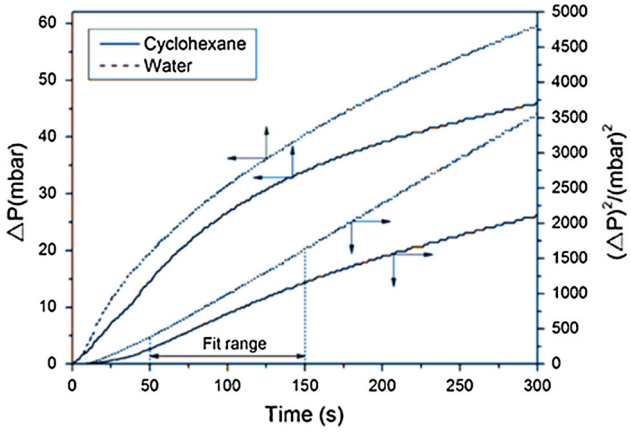

Fig. 10—Pressure difference *vs* time with different liquids.

Table II. Summary of Bond Work Index for VTM

$P(\mu m)$	P_{80} (μm)	F_{80} (μm)	G_{bp} (g/rev)	W_i (KWh/t)
75	120	65	1.061	52.86

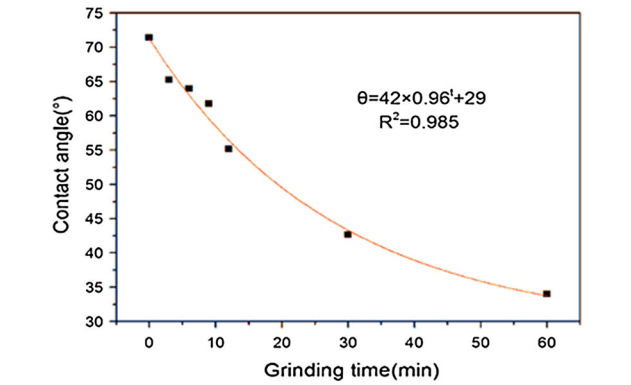

Fig. 11—Contact angle *vs* grinding time.

E. *Moisture Capacity*

Moisture capacity is defined as the maximum water content that can be held by iron ore particles per unit mass.[24] Some research shows that the moisture capacity and optimum water content have a highly positive correlation. Iron ores, which have high moisture capacity, require the addition of more water during the granulation process to achieve high permeability of the granule bed.[25] Figure 12 shows the water content absorbed by the VTM concentrates obtained after grinding for different times as a function of time. The corresponding dependence between the moisture capacity and mass transfer coefficient is shown in Figure 13. The moisture capacity quickly increased when the grinding time was 3 minutes and then continued to change gradually with further increases in grinding time. The mass transfer coefficient increased significantly to reach a maximum at 6 minutes of grinding and then decreased rapidly until the grinding time reached 12 minutes; further increases in grinding time yielded minimal changes in the mass transfer coefficient. The moisture capacity depends to a great extent on the mineral composition and size distribution of the iron ore particles.[23] Among seven samples of identical mineral compositions, only their particle sizes differed. Figure 13 shows that the moisture capacity of the particles increased significantly for the first 3 minutes of grinding, in good agreement with the laser diffraction result showing that the median particle size and mean volume diameter obviously decrease after 3 minutes of grinding (Figure 3).

Two factors influencing the mass transfer coefficient were considered: the wettability and the particle size of the VTM concentrate powders. The Washburn equation relates the capillary increase rate of a liquid through a compact vertical bed of particles via the small pore radius and the contact angle:[26]

$$\frac{dl}{dt} = \frac{r}{\eta}\frac{\gamma}{4l}\cos\theta, \qquad [9]$$

where r is the effective capillary radius, η is the viscosity of the penetrating liquid, γ is the surface tension of

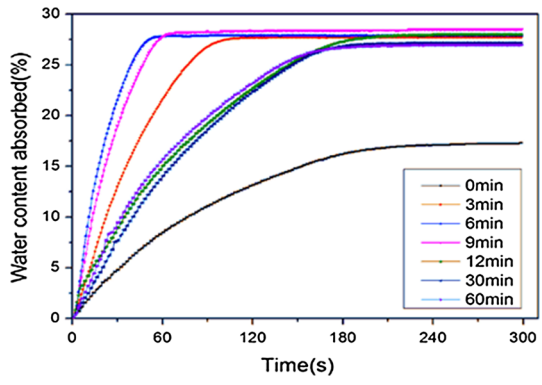

Fig. 12—Water content absorbed *vs* time for materials with different grinding times.

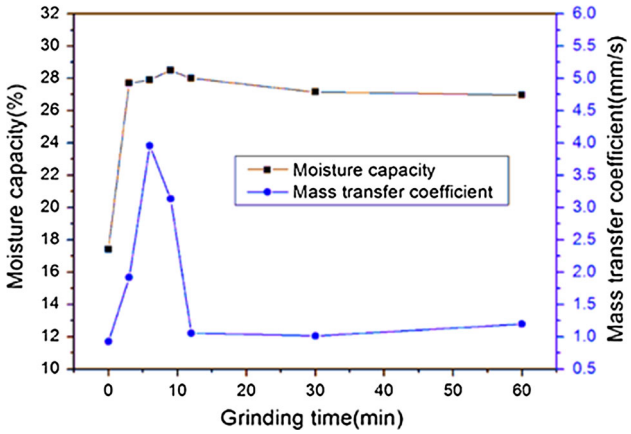

Fig. 13—Moisture capacity and mass transfer coefficient *vs* grinding time.

Table III. Contact Angle for Different Grinding Times

Grinding Time (Min)	0	3	6	9	12	30	60
Contact angle (deg)	71	65	64	62	55	43	34

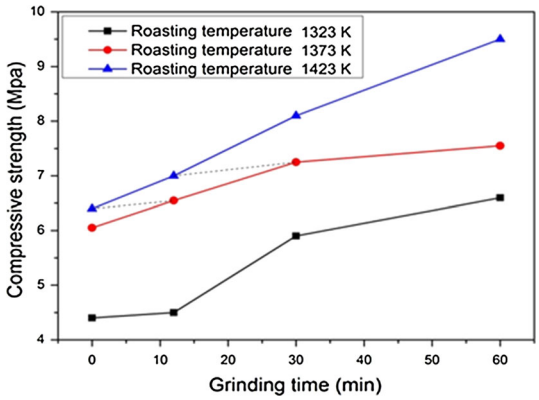

Fig. 14—Compressive strength of finished pellets *vs* grinding time for different roasting temperature (roasting time was 8 minutes for each pellet).

the penetrating liquid, l is the height of liquid penetrating the bed in time t, and θ is the advancing particle contact angle.

The rate at which a liquid penetrates in the particle bed under its own capillary pressure is directly proportional to the radius of the capillary tube and the cosine of the contact angle. The wettability and size distribution determine the advancing particle contact angle and effective capillary radius and, thus, influence the penetration rate. The mass transfer coefficient increased as the contact angle decreased and as the effective capillary radius increased. After the first 6 minutes of grinding, the influence of the wettability of the VTM concentrate powder is greater, and thus, the mass transfer coefficient increased obviously. Then for 6 to 12 minutes, the size distribution plays a dominant role. On the one hand, the effective capillary radius decreases as the size decreases.

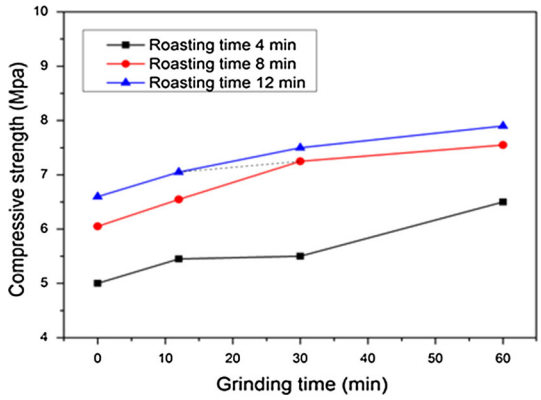

Fig. 15—Compressive strength of finished pellets *vs* grinding time for different roasting time (roasting temperature was 1373 K (1100 °C) for each pellet).

Table IV. Quality of Green Pellets

Index	Drop Numbers/ Times	Compressive Strength/N
Without Damp Mill	4.8	13
With Damp Mill	6.5	16

On the other hand, the connectivity decreases with the increasing fraction of small particles. After 12 minutes, the two factors showed the same effect, and the mass transfer coefficient slightly changed as the grinding time increased.

IV. EFFECT OF GRINDING PROCESS ON PELLETS QUALITY

This section focuses on the effect of grinding time on the strength of baked pellets. Magnetite iron ore green pellets were produced using a tumbling plate at a certain moist content, dried, roasted at high temperature, cooled, and then transported to ironmaking plants. The oxidation reaction of magnetite to hematite is the most characteristic phenomenon in the induration of green iron ore pellets made from magnetite concentrates. As noted in Section III-C, the crystallite size of ground concentrates decreases, whereas their structural microstrain increases with increasing grinding time. These changes can also contribute to the reactivity of magnetite which is oxidized to hematite during the induration process.

The quality of green pellets in the absence/presence of damp mill is presented in Table IV. The drop numbers and the compressive strength of green pellets were improved when the concentrate was pretreated by damp mill. The roasting time and temperature are two important factors that affect pellet quality. The authors aimed to lower the roasting temperature or shorten the roasting time by varying the grinding process. Non-ground and ground (12, 30, and 60 minutes) VTM concentrates were formed into cylinder briquettes under

20 Mpa pressure using a briquette maker. The diameter of the cylinder was 20 mm, and the total mass of the sample was 15 g. Briquette roasting was conducted in an alumina crucible set in a 35 mm electric tube furnace, where the temperature profile was divided into four continuous zones: drying at 393 K (120 °C), preheating at 673 K (400 °C), roasting at 1323 to 1423 K (1050 to 1150 °C), and cooling at about 873 to 1273 K (600 to 1000 °C). The quality indices of pellets are expressed by the compressive strength in MPa of an individual pellet. To measure the compressive strength of a roasted pellet, the pellet is subjected to uniform loading between two parallel plates until it ruptures. Five pellets were measured, and the mean compressive strength at which the pellets broke down was calculated in MPa. Figures 14 and 15 show the compressive strength of finished pellets as a function of grinding time at different roasting temperatures and roasting times. The compressive strength of finished pellets was enhanced by increasing the grinding time. While lowering the roasting temperature and shortening the roasting time through the grinding process appeared to be impossible, longer grinding times can compensate for the effect of lower roasting temperatures on the strength of the pellets. For example, in Figure 14, the strengths of pellets ground for 12 and 30 minutes and roasted at 1373 K (1100 °C) were better than those of pellets ground for 0 and 12 minutes and the roasted at 1423 K (1150 °C). Figure 15 also shows that longer grinding times can compensate for the effects of shorter roasting times on the strength of the pellets. For example, the strength of the pellets ground for 30 minutes and roasted for 8 minutes at 1373 K (1100 °C) were better than that of pellets ground for 12 minutes and roasted for 12 minutes at 1373 K (1100 °C). This finding is of great significance for reducing energy consumption and avoiding ring formation in the kiln during roasting.

V. CONCLUSIONS

The grinding behavior of VTM concentrates in a damp mill was studied, and the principal findings can be summarized as follows:

1. A grinding kinetics equation was established based on a population balance model using size distribution data obtained from a laser diffraction technique $R(x,t) \approx R(x,0)\exp(-0.0056x^{0.95}t^{0.19})$. The further application of the developed models will be used in other types iron ores, such as hematite, magnetite, and siderite.
2. The surface gets rough with increasing the grinding time. Agglomeration of fine particles was enhanced obviously when grinding time reached 30 minutes. The crystallite size of the concentrates decreased from about 673 nm to about 510 nm, whereas their structural microstrain increased from 0.031 pct to about 0.048 pct after 60 minutes of milling.
3. An equation to describe the relationship between the grinding time and contact angle was established: $\theta = 42 \times 0.96^{t} + 29$. The compressive strength of roasted pellets was enhanced by increasing grinding times. Lowering the roasting temperature while shortening the roasting time by grinding appeared to be possible.

ACKNOWLEDGMENTS

The authors are thankful to the Project of National Natural Science Foundation (51504003) and Project of Science and Technology Development Anhui Province (1501041126) and Key Project of Natural Science Research of Universities of Anhui Province (KJ2015A028) for sponsoring the study.

REFERENCES

1. G.H. Bai, X.Q. Zhou, X.H. Fan, and J.C. Li: *J. Cent. South Univ. Sci. Technol.*, 2011, vol. 42, pp. 1509–15.
2. T. Huang, Z.C. Li, Q. Yang, and Y.B. Jiang: *J. Cent. South Univ. Sci. Technol.*, 2004, vol. 35, pp. 753–58.
3. D.Q. Zhu, X.F. Xu, J. Pan, Y. Ou, J. Li, and Y. Tang: *J. Cent. South Univ. Sci. Technol.*, 2007, vol. 38, pp. 843–49.
4. X.B. Huang, X.W. Lv, C.G. Bai, G.B. Qiu, and L.M. Lu: *ISIJ Int.*, 2014, vol. 54, pp. 2721–27.
5. D.Q. Zhu, T.J. Chun, J. Pan, and J.L. Zhang: *Int. J. Min. Process.*, 2013, vol. 125, pp. 51–60.
6. T.J. Chun and D.Q. Zhu: *Metall. Mater. Trans. B*, 2015, vol. 46B, pp. 1–4.
7. C. Frances: *Powder Technol.*, 2004, vol. 143, pp. 253–63.
8. W.S. Choi, H.Y. Chung, B.R. Yoon, and S.S. Kim: *Powder Technol.*, 2001, vol. 115, pp. 209–14.
9. G. Matijasic and S. Kurajica: *Powder Technol.*, 2010, vol. 197, pp. 165–69.
10. Y. Nakajima and T. Tanaka: *Ind. Eng. Chem. Process Des. Dev.*, 1973, vol. 12, pp. 23–25.
11. D.Q. Zhu, J. Pan, L. Lu, and R.J. Holmes: *Iron Ore Pelletization*, Woodhead Publisher, New York, 2015, vol. 15, pp. 435–73.
12. F.C. Bond: *Trans. AIME*, 1952, vol. 193, pp. 484–94.
13. F. Garcia, N. Le Bolay, and C. Frances: *Chem. Eng. J.*, 2002, vol. 85, pp. 177–87.
14. F. Apaydin, A. Atasoy, and K. Yildiz: *Can. Metallurg. Q.*, 2011, vol. 50, pp. 113–18.
15. A.A. Baig, J.L. Fox, R.A. Young, Z. Wang, J. Hsu, W.I. Higuchi, A. Chhettry, H. Zhuang, and M. Otsuka: *Calcif. Tissue Int.*, 1999, vol. 64, pp. 437–49.
16. R. Delhez, T.H. Keijser, and E.J. Mittemeijer: *Fresenius' J. Anal. Chem.*, 1982, vol. 312, pp. 1–16.
17. S. Enzo, G. Fagherazzi, A. Benedetti, and S. Polizzi: *J. Appl. Crystallogr.*, 1988, vol. 21, pp. 536–42.
18. R. Tahmasebi, M. Shamanian, M.H. Abbasi, and M. Panjepour: *J. Alloys Compd*, 2009, vol. 472, pp. 334–42.
19. L. Galet, S. Patry, and J. Dodds: *J. Colloid Interf. Sci.*, 2010, vol. 346, pp. 470–75.
20. A. Siebold, M. Nardin, J. Schultz, A. Walliser, and M. Oppliger: *Colloids Surf. A Physicochem. Eng. Aspects*, 2000, vol. 161, pp. 81–87.
21. T.V. Subrahmanyam, C.A. Prestidge, and J. Ralston: *Min. Eng.*, 1996, vol. 9, pp. 727–41.
22. R.D. Zhang, X.W. Lv, X.B. Huang, and M.J. Zhou: *J. Iron Steel Res.*, 2012, vol. 24, pp. 123–29.
23. R.N. Wenzel: *J. Phys. Chem.*, 1949, vol. 53, pp. 1466–67.
24. X.W. Lv, C.G. Bai, G.B. Qiu, S.F. Zhang, and M.L. Hu: *ISIJ Int.*, 2010, vol. 50, pp. 695–701.
25. X.W. Lv, C.G. Bai, C.Q. Zhou, H. Xie, and R.M. Shi: *Ironmak. Steelmak.*, 2010, vol. 37, pp. 407–13.
26. E.W. Washburn: *Phys. Rev.*, 1921, vol. 17, p. 273.